Journal of
Nanoscience and Nanotechnology
Vol. 10, 1–7, 2010

J. Nanosci. Nanotechnol.10, 6683-6690,2010

Scratch Resistance of Polycarbonate Containing ZnO Nanoparticles: Effects of Sliding Direction

María Dolores Bermúdez[1], Witold Brostow[2,*], Francisco J. Carrión-Vilches[1,2,*], and José Sanes[1]

[1] *Grupo de Ciencia de Materiales e Ingeniería Metalúrgica, Departamento de Ingeniería de Materiales y Fabricación, Universidad Politécnica de Cartagena, Campus de la Muralla del Mar, C/ Doctor Fleming s/n. 30202-Cartagena, Spain*
[2] *Laboratory of Advanced Polymers & Optimized Materials (LAPOM), Department of Materials Science and Engineering, University of North Texas, 1150 Union Circle # 305310, Denton, TX 76203-5017, USA*

Abrasive wear resistance of injection molded polycarbonate (PC) and polycarbonate + zinc oxide nanocomposites containing 0.5 wt% ZnO nanoparticles was determined as a function of the sliding direction with respect to injection flow. First we have done single scratch testing under progressively increasing the load applied. Then sliding wear testing consisting of 15 successive scratches along the same groove was performed. Neat PC shows anisotropic behavior, with instantaneous penetration depth more than 50% higher in the direction parallel to the melt injection flow than in the transverse direction. Viscoelastic recovery after scratching of neat PC is also higher in the longitudinal than in the transverse direction, hence final residual depth values are similar in both directions. The addition of ZnO nanoparticles reduces the instantaneous penetration depth in the longitudinal direction but lowers viscoelastic recovery so that the residual depth is large. In the transverse direction, the scratch resistance is similar for neat PC and the nanocomposite. Dynamic mechanical analysis, SEM/FIB results and wear mechanisms from SEM observations of wear scars are discussed. Below the glass transition region the nanocomposite has distinctly higher storage modulus E' than PC—a clear reinforcement effect. However, the addition of ZnO nanoparticles to the polymer increases the material brittleness at room temperature by a factor of 2.72.

Keywords: Polycarbonate, Zinc Oxide Nanoparticles, Scratch Resistance, Brittleness, Anisotropy.

RESEARCH ARTICLE

1. INTRODUCTION

Improvement of tribological performance and surface stability of polymer based materials (PBM) is an important factor to increase their service lifetime. This is particularly important in a growing number of applications where PBM replace metals. Among other types of permanent damage, *abrasive wear* leads to the loss of finishing and optical properties.

The most frequent approaches to improve polymer tribological performance include the use of coatings, blending of polymers and addition of fillers-in particular, ceramic nanoparticles.[1–22] There has already been some work on ZnO nanocomposites.[1, 6, 14, 16]

Since the surface properties of polymers may be different from those of the bulk, scratch resistance tests provide a useful measure of abrasive wear. This is particularly true in sliding wear determination (repetitive scratching along the same groove) or under increasingly severe load and velocity sliding conditions.[10–12, 23, 24]

Polycarbonate (PC) is an amorphous engineering thermoplastic with good processibility, low density, high transparency and strength. It is the material of choice for applications such as covers of automotive displays, optical lenses and eyeglasses. Service requirements include an improvement of the scratch resistance as well as high stability under severe environmental conditions.

New polycarbonate nanocomposites[13, 14, 16, 17] are being developed in order to improve the thermal, mechanical, electrical or optical properties of the base polymer.

Our previous work[16, 17] on tribological properties of polycarbonate + ZnO nanocomposites has shown that 0.5 wt% content of ZnO nanoparticles reduces the wear rate of polycarbonate by 76% under a pin-on-disk con-

*Authors to whom correspondence should be addressed.

figuration against steel. A good tribological performance of PC + 0.5% ZnO nanocomposite is also found under a thrust-washer contact geometry, where the composite shows higher load-carrying capacity than polycarbonate, reducing both the wear rate and the dynamic friction against steel. Given the critical role of scratch resistance of PC in many technological and structural applications, we now compare the abrasive wear resistance of our nanocomposite with that of neat PC under variable scratching conditions. Scratch resistance anisotropy has been observed in machined biaxially oriented polymers.[25] In the present work the use of injection molded specimens in scratch and wear testing allows to evaluate the influence of the sliding direction with respect to the injection flow.

2. EXPERIMENTAL DETAILS

2.1. Starting Materials

Polycarbonate (PC) with a molecular weight of $2.2{\cdot}10^4$ was supplied by Kotec Corporation, Osaka, Japan. ZnO nanoparticles with an average particle size of 53 nm were supplied by Sigma-Aldrich and have been used before.[16, 17, 26]

2.2. Materials Preparation

The polymer was mixed with the corresponding proportion of ZnO nanopowder filler in an ultracentrifugal mill at 18000 rpm during 30 s. After heating at 110 °C for 8 hours, tensile test coupons (according to ASTM D-256) and discs (Fig. 1) of neat PC or the nanocomposite were simultaneously injection molded at 280 °C and 9 MPa in a DEU (Spain) 250H55 mini VP injection machine with a mold temperature of 80 °C and a holding pressure of 9 MPa. A final surface roughness ($R_a \leq 0.8$ μm) was found. SEM and EDS characterization of PC+ZnO blends have been reported earlier.[16, 17]

2.3. Dynamic Mechanical Analysis

Dynamic mechanical analysis (DMA) was carried out using a Q800 de TA Instruments equipment under the single cantilever mode from 25 °C to 170 °C, at a heating rate of 3 °C/min, at an oscillatory frequency of 1.0 Hz under a 1.0% strain on samples of dimensions $17.4 \times 4.1 \times 3.1$ mm obtained from injected discs (Fig. 1). The DMA technique has been described by Lucas and her colleagues[27] and also by Menard.[28]

2.4. Scanning Electron Microscopy (SEM)

SEM images were obtained using a Hitachi S3500N scanning microscope. The samples were sputter coated with a thin layer of gold in order to make them conductive with the aid of a SC7640 Sputter Coater of Polaron Division.

2.5. Focused Ion Beam (FIB) and Field Emission Scanning Electron Microscopy (FESEM)

A FEI Nova 200 Dual Beam apparatus comprising FIB and FESEM was used to obtain cross-sections of our nanocomposite. The combination was described in Ref. [29] FIB was used at 17 nA probe current and 15 kV accelerating voltage. Micro-sections with dimensions of $6 \times 5 \times 5$ mm took 20 minutes at 52° of tilt, followed by 2 cycles of cleaning for 40 s.

2.6. Friction Tests

Static and dynamic friction values were recorded for polymer discs (Fig. 1) sliding against stainless steel sheet according to ASTM D 1894 standard using a mechanical testing machine (Hounsfield H25KS) with a sliding velocity of 150 mm/min; the load was 392 g and the sliding distance = 150 mm.

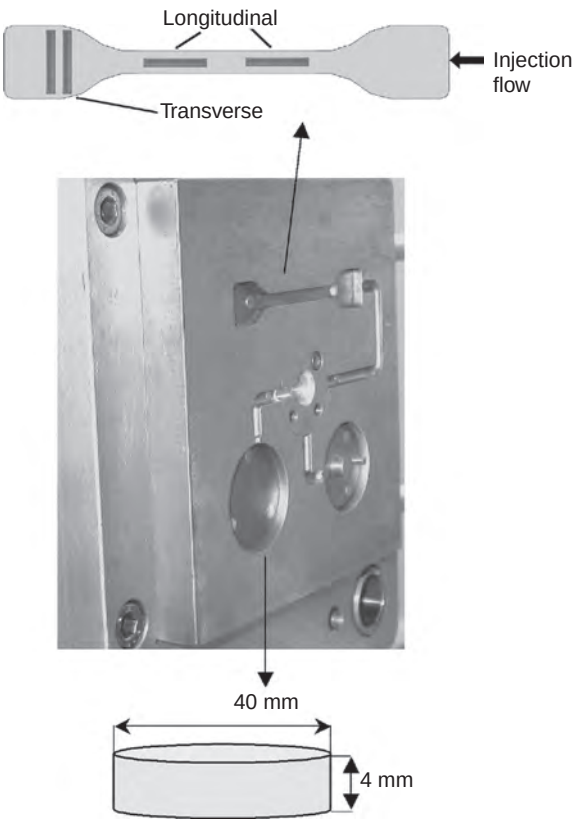

Fig. 1. Injection molding chamber: tensile coupons used for scratch tests; disc used for DMA and friction tests.

RESEARCH ARTICLE

2.7. Scratch Testing

Scratch tests were carried out on tensile test specimens (Fig. 1) using a CSM Micro-Scratch Tester (MST) equipped with a conical diamond indenter (200 mm diameter and 120° cone angle) following the procedure described in detail before.[4, 30] The scratch length was 5.0 mm and all tests were carried out at room temperature. Sliding wear was determined by 15 scratches along the same groove performed at 5.0 mm/min under a constant normal load of 2.5 N. Scratch tests under progressively increasing load between 0.03 N and 29.0 N were carried out at 2.5 mm/min. For each test, the instantaneous penetration depth R_p and the residual depth R_h after healing were recorded. Repeated experiments have confirmed that the shallower residual depth in our viscoelastic materials is reached inside 2 min. Therefore, R_h values have in each case been determined inside 2 minutes after recording the R_p values. The percentage of viscoelastic recovery f is calculated as

$$f = [1 - (R_h/R_p)] \times 100 \quad (1)$$

3. DISTRIBUTION OF NANOPARTICLES IN THE MATRIX

The use of unmodified ZnO nanoparticles with a high surface area for the preparation of the nanocomposite described here could give rise to a non-uniform distribution and promote the formation of aggregates, as already reported[14] and seen in the FIB-SEM images in Figure 2. These aggregates could be responsible for the higher brittleness (see below) and the lower chain mobility. In fact, the tribological performance of our nanocomposite can be improved by adding an ionic liquid,[16] which modifies the ZnO nanoparticles.[18]

4. DYNAMIC MECHANICAL PROPERTIES

Figure 3 shows the evolution of storage modulus E', the loss modulus E'' and tan $\delta = E''/E'$ with temperature for neat PC and the nanocomposite. The onset values of the storage modulus fall and the maximum loss modulus and tan δ values are listed in Table I.

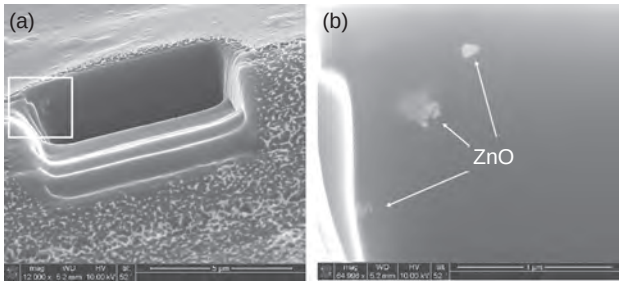

Fig. 2. FIB-SEM images of the nanocomposite showing ZnO nanoparticles in the PC matrix: (a) ×12000 (b) ×65000.

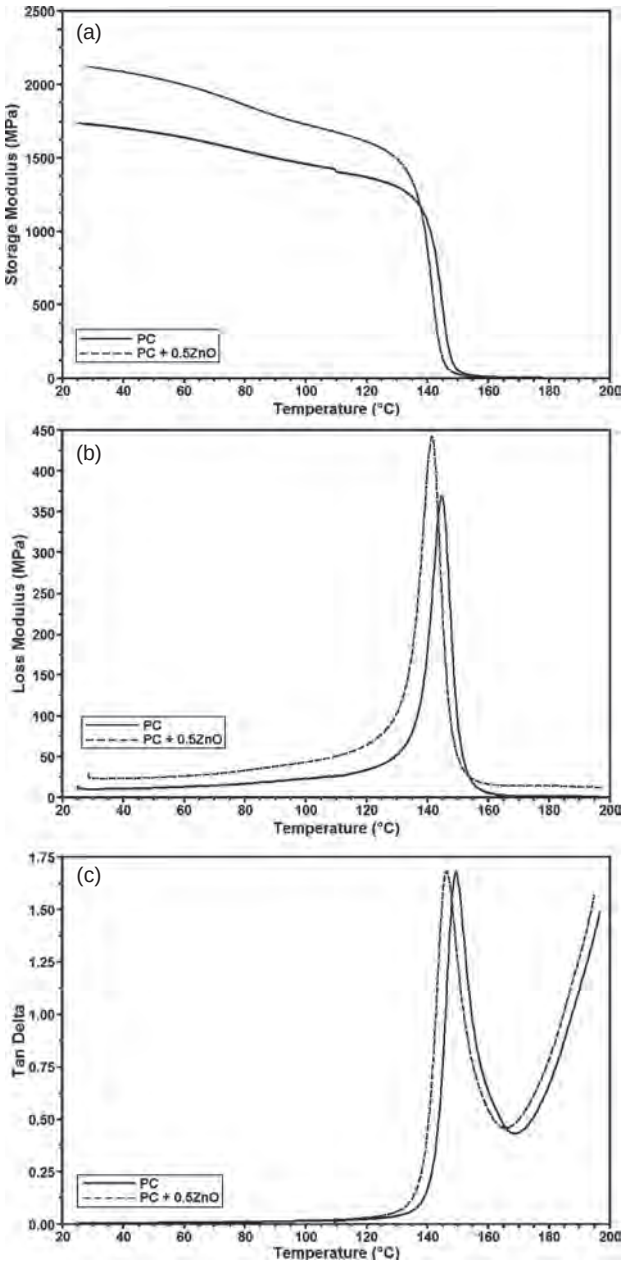

Fig. 3. DMA properties of PC and the nanocomposite as a function of temperature: (a) storage modulus E'; (b) loss modulus E''; (c) tan δ.

The present results are in agreement with previously reported[14] decrease of the elongation at break ε_b. The presence of ZnO nanoparticles increases the brittleness of PC and reduces its thermal stability; brittleness of materials has been defined[23] as

$$B = 1/(\varepsilon_b E') \quad (2)$$

From our results at room temperature $B = 0.106$ for PC and 0.289 for our nanocomposite.

RESEARCH ARTICLE

J. Nanosci. Nanotechnol.10, 6683-6690,2010

Table I. Dynamic mechanical properties of PC and the nanocomposite.

	Storage modulus (Onset of fall)		Loss modulus (Peak)		tan δ (Peak)	
Material	T/(°C)	E'/(MPa)	T/(°C)	E'/(MPa)	T/(°C)	E''/E'
PC	140.2	1056	144.6	368.7	149.5	1.678
Nanocomposite	136.6	1260	141.7	429.8	146.3	1.683

In Table I we also see that the fall of E' in the glass transition region begins at a lower temperature for the nanocomposite than for neat PC. Apparently perturbation of the structure of the neat polymer by the presence of Zn particles moves the onset of the glass transition somewhat downwards. An analysis of methods of location of the glass transition has been performed;[31] the recommendation is that the glass transition temperature T_g is best located in the middle of the E' fall region. We see in Figure 3 that the fall region for the nanocomposite is significantly larger than for the PC; the ZnO particles have pushed E' at low temperatures upwards, an expected effect, hence a larger fall. Thus, the midpoints of both regions are close to one another. We note that variations of T_g with composition for polymer + polymer[32] and also for polymer + drug systems[33] can be described by an analytical equation.

5. FRICTION

Table II shows the static and dynamic friction values in the absence of wear recorded for PC and the nanocomposite sliding against stainless steel. The addition of ZnO *reduces the static* friction of PC by ≈15%. Once the steady state is reached, both materials show similar dynamic friction. The influence of the presence of ZnO nanoparticles on the dynamic friction of PC under wear conditions[14] depends on the contact configuration: pin-on-disc results are similar for PC and the nanocomposite, while thrust-washer tests show a strong friction reduction for the latter.

6. SCRATCH RESISTANCE AND SLIDING WEAR

6.1. Progressive Load Tests

Figure 4 shows R_p and R_h values for both materials under single scratching when the normal applied load increases from approximately 0.03 N to 29 N, as a function of sliding direction with respect to the injection flow (see again Fig. 1). Table III shows R_p, R_h and viscoelastic recovery values under the highest applied load.

Table II. Static and dynamic friction of PC and PC + the nanocomposite (standard deviation in parenthesis).

Material	Static friction	Dynamic friction
PC	0.27 (0.0096)	0.17 (0.010)
Nanocomposite	0.23 (0.0080)	0.18 (0.0043)

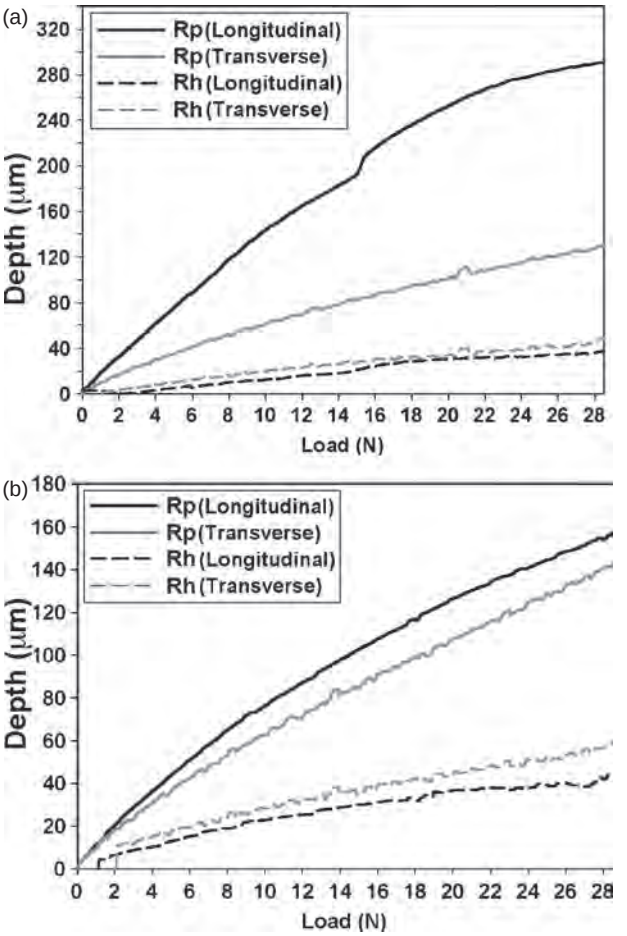

Fig. 4. Penetration depth and residual depth value under progressively increasing load: (a) PC; (b) nanocomposite.

As expected, as load increases, the depth values increase. However, there is a remarkable influence of sliding direction on the penetration depth (R_p) values for neat PC: a 55% R_p increase in the longitudinal direction with respect to the transverse direction under the highest applied load. By contrast, the composite only shows a 9.9% increase in R_p in the longitudinal direction with respect to R_p in the transverse direction, also under the highest load. Both materials show a similar variation of R_h with sliding direction, with a 23% increase in the transverse direction with respect to the longitudinal one under the highest applied load. These results show that the viscoelastic recovery for neat PC is much higher in the longitudinal direction (88%) than in the transverse one (62.5%), while this anisotropic behavior is reduced by the presence of ZnO nanoparticles, to 71% and a 58.5%, respectively. Apparently, the presence of the ceramic particles hampers viscoelastic recovery of the chains.

In order to understand the mechanisms responsible for this highly anisotropic behavior of neat PC, scratching scars were observed under SEM. Figure 5(a) shows the

J. Nanosci. Nanotechnol.10, 6683-6690,2010

RESEARCH ARTICLE

Table III. Scratch resistance under progressive load.

	Sliding direction					
	Longitudinal			Transverse		
Material	Penetration depth $R_p/(\mu m)$	Residual depth $R_h/(\mu m)$	Viscoelastic recovery $f/(\%)$	Penetration depth $R_p/(\mu m)$	Residual depth $R_h/(\mu m)$	Viscoelastic recovery $f/(\%)$
PC	292.8	37.5	87.7	130.2	48.8	62.5
Nanocomposite	157.3	45.9	70.8	143.1	59.4	58.5

scars on neat PC in the transverse and longitudinal directions, respectively. The longitudinal scar tip on neat PC (Fig. 5(b)) shows a smooth crack-free appearance and the presence of wear debris particles. When the scar tip on the nanocomposite in the longitudinal direction (Fig. 5(d)) is observed, a cracking mechanism appears with cracks perpendicular to the sliding direction. This cracking mechanism is not present in neat PC under the same conditions (Fig. 5(b)) and could be due to the more brittle behavior of the nanocomposite. We recall that at 25 °C $B = 0.106$ for PC and 0.289 for our nanocomposite.

The highest chain mobility of PC in the longitudinal direction would explain the highest penetration depth and viscoelastic recovery values.

In the transverse direction, the scar surfaces of PC and the nanocomposites (Figs. 5(c) and (e), respectively) show the presence of microcracks perpendicular to the sliding direction which cross the entire scratch groove and are a prolongation of the surface texture present outside the scar. Such as deformation mechanism would explain the more uniform viscoelastic response of both materials in the transverse direction (see Table III).

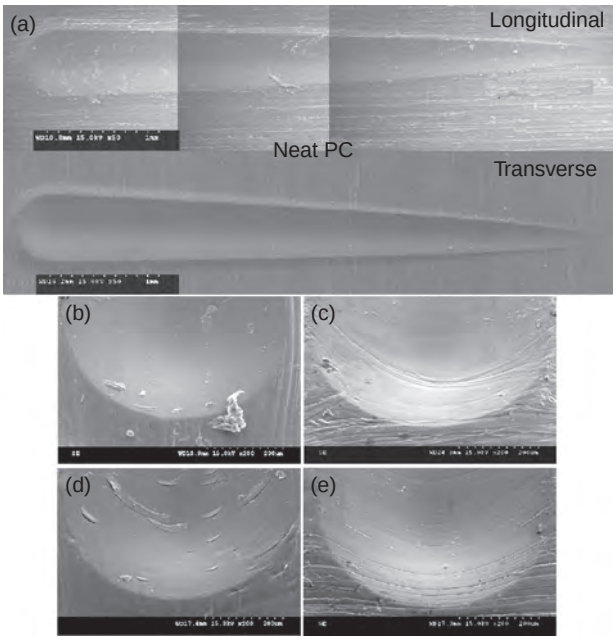

Fig. 5. SEM micrographs of the scratch grooves under progressive load: (a) PC as a function of direction; (b) Scratch tip on PC (longitudinal); (c) Scratch tip on PC (transverse); (d) Scratch tip on the nanocomposite (longitudinal); (e) Scratch tip on the nanocomposite (transverse).

6.2. Sliding Wear

Figure 6 shows the penetration depth and residual depth values for PC and the composite as a function of the number of scratches along the same groove; the indenter slides parallel or perpendicular to the injection flow. Values after 15 scratches are listed in Table IV.

As has been previously described[10, 11] for other thermoplastic materials, the increase of depth values with each

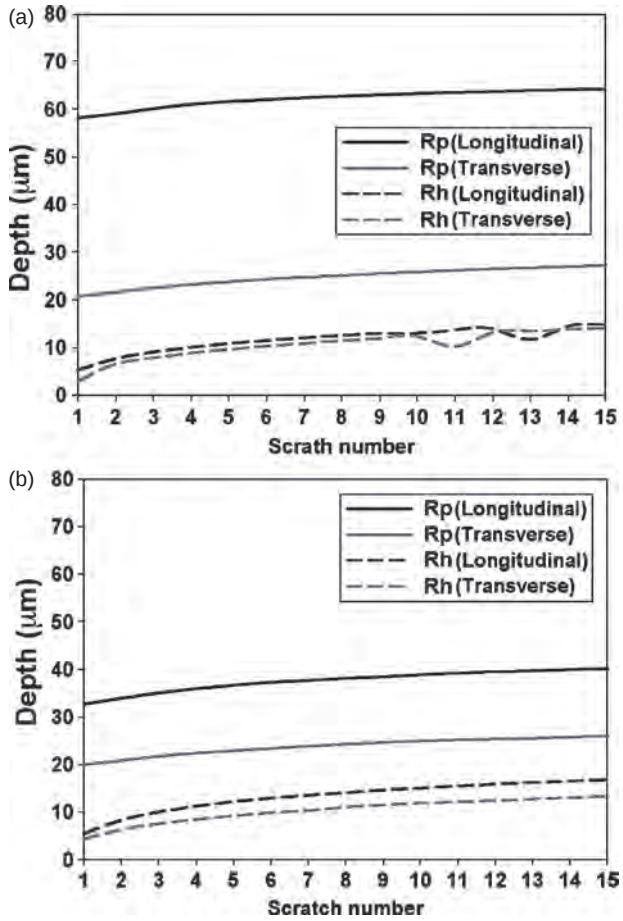

Fig. 6. Penetration and residual depth values in sliding wear determination as a function of the number of scratches and the sliding direction: (a) PC; (b) nanocomposite.

J. Nanosci. Nanotechnol.10, 6683-6690,2010

Table IV. Sliding wear results.

	Sliding direction					
	Longitudinal			Transverse		
Material	Penetration depth $R_p/(\mu m)$	Residual depth $R_h/(\mu m)$	Viscoelastic recovery $f/(\%)$	Penetration depth $R_p/(\mu m)$	Residual depth $R_h/(\mu m)$	Viscoelastic recovery $f/(\%)$
PC	64.3	14.7	77.1	27.2	14.1	48.2
Nanocomposite	40.16	16.8	58.2	26.0	13.4	48.5

new scratch on the same groove is lower as the number of scratches increases. This has been attributed to a strain hardening effect which is found in most thermoplastics-with the notable exception of polystyrene.[23]

Again, neat PC shows a clear anisotropic behavior, with a penetration depth value a 64% higher in the longitudinal than in the transverse direction after a single scratch, and a 68% higher after 15 scratches. The residual depth in the longitudinal direction is also a 45% higher than in the transverse direction after a single scratch, but this difference is reduced or disappears after 10 scratches. As a result, a 77% viscoelastic recovery is reached after 15 scratches in the longitudinal direction, and only a 48% in the transverse direction. This anisotropy is again reduced in the case of the nanocomposite, with a 58% viscoelastic recovery in the longitudinal direction and a 48% in the transverse one.

The scratch behavior of both materials in the transverse direction is very similar. The presence of ZnO nanoparticles induces only a slight reduction (5%) in the residual depth value after 15 scratches in the transverse direction with respect to neat PC, the viscoelastic recovery is similar for both materials.

Figure 7 shows that for neat PC the longitudinal multiscratching groove (Fig. 7(a)) presents a smooth surface with some wear debris particles adhered to it. In the transverse direction (Fig. 7(b)) microcracks propagate from the outer surface texture and cross the scar perpendicularly to the sliding direction. The repeated sliding of the indenter along the same groove in the longitudinal direction produces an accumulation of plastically deformed layers-as can be observed in a SEM micrograph of the scar edge under a higher magnification (Fig. 7(c)) for neat PC. For the nanocomposite the scar edge after 15 scratches (Fig. 7(d)) shows a fractured surface. This is in agreement with the more brittle response of this material, and agrees with the lower viscoelastic recovery of the nanocomposite in the longitudinal direction.

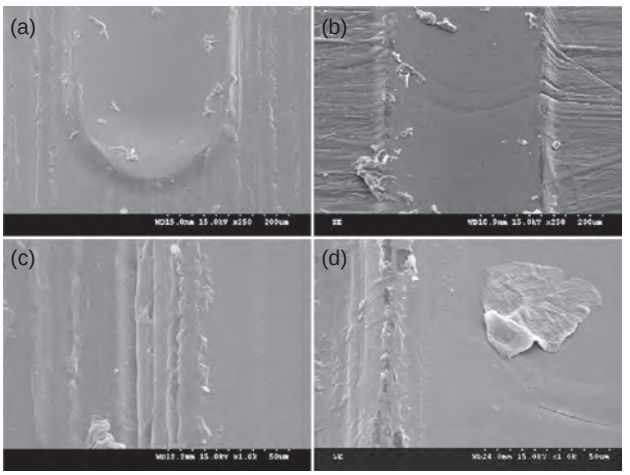

Fig. 7. Sliding wear surfaces: (a) longitudinal scar on PC; (b) transverse scar on PC; (c) scar edge on PC; (d) scar edge on nanocomposite.

It has been suggested,[9] that interactions between chains in the polymer network may play an important role in the abrasive wear resistance of polycarbonate. The molecular mobility of the polymer chains depends on the free volume. Earlier,[23, 24] we have demonstrated a relationship between the scratch resistance of polymers and their free volume and brittleness. It is well known[34] that the orientation in an injection molded polymer varies over the cross section and along the flow. The elongation at break and stiffness are generally higher in the direction parallel to the orientation than in the direction perpendicular to it.

Under conventional tensile test,[14] our nanocomposite shows a 73% reduction in elongation at break with respect to neat PC; thus a lower viscoelastic recovery should be expected for the nanocomposite than for the neat polymer. In the case of neat polycarbonate, the enhanced chain slippage in the longitudinal direction would favor the deformation and recovery processes due to chain mobility.

In a similar way, the presence of ZnO nanoparticles within the polycarbonate matrix could reduce its ability to absorb the applied stress due to interactions between the large surface area nanoparticles and the polymer chains, thus limiting the slippage of the chains and leading to a more brittle failure. This apparently accounts for a similar response of both materials under scratching in the transverse direction.

Under severe wear damage of the pin-on-disc and thrust-washer contact conditions,[14] the degree of viscoelastic recovery is negligible, higher hardness and stiffness of the nanocomposite are responsible for the improved tribological performance.

RESEARCH ARTICLE

7. A SURVEY OF RESULTS

The scratch resistance of polycarbonate depends on the sliding direction with respect to polymer chain orientation with injection flow. Under the experimental conditions studied here, the viscoelasic recovery of polycarbonate is higher in the longitudinal (parallel to the injection flow) than in the transverse (perpendicular to the injection flow) direction.

The addition of a 0.5 wt.% of ZnO nanoparticles increases the storage modulus and reduces the glass transition temperature of polycarbonate.

The effect of ZnO nanoparticles on the scratch resistance of polycarbonate depends on experimental conditions, but always reduces the anisotropic behavior of PC with sliding direction due to interactions between the nanoparticles and the polymer network.

The different response with sliding direction found in PC and the nanocomposite are related to the deformation mechanisms that operate in each case. In agreement with its higher brittleness, the nanocomposite always shows a cracking mechanism, while neat PC shows cracking only in the transverse direction.

Acknowledgments: We wish to thank MICINN (Spain) and the EU FEDER program (MAT2008-01670) and Programa de Generación de Conocimiento Científico de Excelencia, Fundación Séneca Región de Murcia (Spain), (08596/PI/08) for financial support. Francisco J. Carrión is grateful to Fundación Séneca for a grant under the program "Estancias Externas de Investigadores de la Región de Murcia." A partial support by the Robert A. Welch Foundation (Grant #B-1203) is also acknowledged.

References and Notes

1. S. Bahadur, L. Zhang, and J. W. Anderegg, *Wear* 203/204, 464 (**1997**).
2. M. Rabello, Aditivação de Polimeros, Artliber, São Paulo (**2000**), Chap. 10.
3. W. G. Sawyer, K. D. Freudenberg, P. Bhimaraj, and L. S. Schadler, *Wear* 254, 573 (**2003**).
4. W. Brostow, J.-L. Deborde, M. Jaklewicz, and P. Olszynski, *J. Mater. Ed.* 25, 119 (**2003**).
5. L. Rapoport, O. Nepomnyashchy, A. Verdyan, R. Popovitch-Biro, Y. Volovik, B. Ittah, and R. Tenne, *Adv. Eng. Mater.* 6, 44 (**2004**).
6. A. Moustaghfir, A. Rivaton, E. Tomasella, B. Mailhot, J. Cellier, M. Jacqet, and J. L. Gardette, *J. Appl. Polym. Sci.* 95, 380 (**2005**).
7. N. K. Myshkin, M. I. Petrokovets, and A.V. Kovalev, *Tribol. Internat.* 38, 910 (**2005**).
8. W. Brostow, M. Keselman, I. Mironi-Harpaz, M. Narkis, and R. Peirce, *Polymer* 46, 5058 (**2005**).
9. Y. J. Mergler, R. J. van Kampen, W. J. Nauta, R. P. Schaake, B. Raas, J. G. H. van Griensven, and C. J. M. Meesters, *Wear* 258, 915 (**2005**).
10. M. D. Bermudez, W. Brostow, F. J. Carrion, J. J. Cervantes, and D. Pietkiewicz, *Polymer* 46, 347 (**2005**).
11. M. D. Bermudez, W. Brostow, F. J. Carrion, J. J. Cervantes, and D. Pietkiewicz, *e-Polymers* 001 (**2005**).
12. M. D. Bermudez, W. Brostow, F. J. Carrion, J. J. Cervantes, G. Darmarla, and J. M. Perez, *e-Polymers* 003 (**2005**).
13. J. Sanes, F. J. Carrion, and M. D. Bermudez, *e-Polymers* 005 (**2007**).
14. F. J. Carrion, J. Sanes, and M. D. Bermudez, *Wear* 262, 1504 (**2007**).
15. T. E. Twardowski, Introduction to Nanocomposite Materials, DEStech, Philadelphia (**2007**).
16. F. J. Carrion, J. Sanes, and M. D. Bermudez, *Mater. Lett.* 61, 4531 (**2007**).
17. F. J. Carrion, A. Arribas, M. D. Bermudez, and A. Guillamon, *Eur. Polymer J.* 44, 968 (**2008**).
18. F. J. Carrion, M. D. Bermudez, and J. Sanes, Progress on Nanoparticles Research, Nova Science Publishers, New York (**2008**).
19. L. F. Giraldo, W. Brostow, E. Devaux, B. L. Lopez, and L. D. Perez, *J. Nanosci. Nanotechnol.* 8, 3176 (**2008**).
20. W. Brostow, A. Buchman, E. Buchman, and O. Olea-Mejia, *Polymer Eng. Sci.* 48, 1977 (**2008**).
21. A. Arribas, M.-D. Bermudez, W. Brostow, F. J. Carrion-Vilches, and O. Olea-Mejia, *Express Polymer Letters* 3, 621 (**2009**).
22. A. F. Vargas, W. Brostow, H. E. H. Lobland, B. L. Lopez, and O. Olea-Mejia, *J. Nanosci. Nanotechnol.* 9, 6661 (**2009**).
23. W. Brostow, H. E. H. Lobland, and M. Narkis, *J. Mater. Res.* 21, 2422 (**2006**).
24. W. Brostow and H. E. H. Lobland, *Polym. Eng. Sci.* 48, 1982 (**2008**); W. Brostow and H. E. H. Lobland, *J. Mater. Sci.* DOI 10.1007/s10853-009-3926-5.
25. H. Y. Nie, M. J. Walzak, and N. S. McIntyre, *Appl. Surf. Sci.* 253, 2320 (**2006**).
26. J. Sanes, F. J. Carrion, and M. D. Bermudez, *Appl. Surf. Sci.* 255, 4859 (**2009**).
27. E. F. Lucas, B. G. Soares, and E. Monteiro, Caracterização de Polímeros, e-papers, Rio de Janerio (**2001**).
28. K. P. Menard, Dynamic Mechanical Analysis, 2nd edn., CRC Press, Boca Raton, FL (**2008**).
29. W. Brostow, B. P. Gorman, and O. Olea-Mejia, *Mater. Letters* 61, 1333 (**2007**).
30. W. Brostow, B. Bujard, P. E. Cassidy, H. E. Hagg, and P. E. Montemartini, *Mater. Res. Innovat.* 6, 7 (**2002**).
31. W. Brostow, S. Deshpande, D. Pietkiewicz, and S. R. Wisner, *e-Polymers* 109 (**2009**).
32. W. Brostow, R. Chiu, I. M. Kalogeras, and A. Vassilikou-Dova, *Mater. Letters* 62, 3152 (**2008**).
33. R. J. Babu, W. Brostow, I. Kalogeras, and S. Sathigari, *Mater. Letters* 63, 2666 (**2009**).
34. K. Engelsing and G. Menning, *Mech. Time-Dependent Mater.* 5, 27 (**2001**).

Received: 1 September 2009. Accepted: 24 November 2009.

RESEARCH ARTICLE